Plasmonic and magnetoplasmonic interferometry for sensing

New Journal of Physics
The open access journal for physics

Plasmonic and magnetoplasmonic interferometry for sensing

D Martín-Becerra[1,2], G Armelles, M U González and A García-Martín[2]

IMM-Instituto de Microelectrónica de Madrid (CNM-CSIC), Isaac Newton 8, PTM, E-28760 Tres Cantos, Madrid, Spain
E-mail: diana.martin@imm.cnm.csic.es and antonio@imm.cnm.csic.es

New Journal of Physics **15** (2013) 085021 (16pp)
Received 17 May 2013
Published 22 August 2013
Online at http://www.njp.org/
doi:10.1088/1367-2630/15/8/085021

Abstract. The use of plasmonic and magnetoplasmonic interferometers as refractometric-based sensors is studied theoretically, and their performance compared to that of the most commonly used plasmonic sensing technique, the surface plasmon resonance (SPR) sensor. The analysis is based on the evolution with the refractive index of the physical parameters involved for each kind of sensor, as well as the behaviour of the actual measured quantity. Two kinds of sensing configurations, two-dimensional surface and three-dimensional bulk, are considered, and the spectral dependence of the three systems is also taken into account. We show that, although the plasmonic interferometer and the SPR system are based on the same physical parameter, namely the surface plasmon polariton (SPP) wavevector, the first offers better properties as its final sensitivity depends on the interferometer size and can thus be increased by its enlargement. For the magnetoplasmonic interferometer, on the other hand, a new physical parameter participates—the modulation of the SPP wavevector induced by an external applied magnetic field. This new parameter has a higher sensitivity to the refractive index than the SPP wavevector, so monitoring it can lead to sensors with increased properties.

[1] Also at International Iberian Nanotechnology Laboratory, 4710-229 Braga, Portugal.
[2] Authors to whom any correspondence should be addressed.

Contents

1. Introduction

Surface plasmon resonances (SPRs) are commonly used for sensing due to their high sensitivity to changes occurring at the interface in which they take place. Although in previous years there have been several advancements in the use of metallic nanoparticles supporting localized surface plasmons for sensing applications [1–3], traditionally the term SPR sensors denotes those based on thin films with propagating surface plasmon polaritons (SPPs). In fact, SPR sensors are one of the most popular sensing methods, commercialized by several companies, and they are applied in many areas [4, 5], label-free biosensing being one of the most attractive [6]. Nowadays, the main goals in the development of SPR sensors lie within the improvement of the sensitivity and the limit of detection [7], as well as miniaturization [8]. Within this context, some variations of the standard SPR technique have been developed, introducing, for example, magnetic field [9] or photonic waveguides [10].

Interferometry is known as a very sensitive and reliable technique for different applications, and in particular for sensing and biosensing [11, 12]. It constitutes an important route for developing compact integrated sensors, such as Mach–Zehnder configurations in silicon [13] or polymer [14]. Interferometry based sensors have already been compared to SPR techniques, and the former have demonstrated higher sensitivity in most situations [11]. However, SPR sensors are still highly competitive, taking into account the ease of their use and the extended knowledge of immobilization protocols in gold. Recently, both interferometry and plasmonics have been put together in the so-called plasmonic interferometers [15–17]. In fact, plasmonic interferometry for sensing has also been demonstrated, both theoretically and experimentally, in different configurations [18–24]. Although these works show that the plasmonic interferometers offer a good performance as sensors, a direct comparison with the traditional SPR configuration has not been carried out yet.

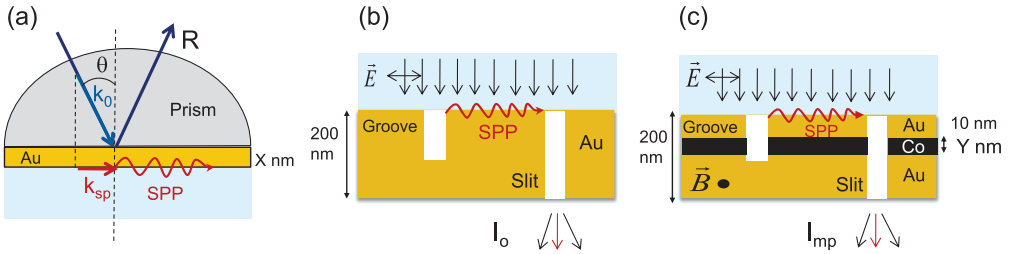

Figure 1. (a) Schematic representation of the traditional SPR configuration. The thickness of the gold layer, X, ranges from 32 to 50 nm depending on the wavelength. (b) Sketch of the plasmonic interferometer. (c) Schema of the MP interferometer. The thickness of the Co layer, Y, depends on the wavelength, varying from 5 to 10 nm.

On the other hand, modulation techniques are usually applied to increase the signal-to-noise ratio in small signals and can be employed to increase the limit of detection and the sensitivity for different sensing systems. In particular, for SPR systems, mechanical [25], phase [26] or magnetic field modulations [9, 27] have been implemented, demonstrating an increase in sensitivity compared to non-modulated configurations. Plasmonic interferometers also allow the introduction of modulated configurations, such as all-optical [16] or electrooptical [28]. Nevertheless, these modulations are originated at the dielectric material, and are therefore not suitable for sensing applications since the dielectric constitutes the sensing material or analyte. Magnetically modulated plasmonic interferometers have also been demonstrated [29], and in this case the active material is a ferromagnetic metal, which avoids the aforementioned problem. Moreover, the magnetic modulation of the SPP presents quite a large dependence on the refractive index of the dielectric material [30], which indicates that magnetoplasmonic (MP) interferometers are a promising tool for sensor development.

Following the path inspired by these results, in this paper we propose the use of MP interferometers as sensing devices, and we theoretically analyse their sensitivity compared to plasmonic (non-magnetic) interferometers. Moreover, we first carry out a detailed comparison of the latter with the traditional SPR technique.

2. General description of sensing layers and methodology

As mentioned in the introduction, three sensing techniques will be compared: SPR, plasmonic interferometry and MP interferometry. All the analysis has been carried out on a numerical basis using a transfer matrix formalism that includes magneto-optical effects [31, 32].

In figure 1 we show schematically the three compared sensing techniques. SPR (figure 1(a)) is based on exciting a surface plasmon in a thin metallic layer (usually ∼50 nm Au layer) by means of attenuated total reflection (ATR) configuration and measuring the corresponding minimum in the reflectivity R. Both interferometries (figures 1(b) and (c)), on the other hand, require a thick metallic layer (usually ∼200 nm thick) and a defect such as a groove to launch the SPP. They are based on the existence of interferences between the SPP and the light directly transmitted through a slit cutting the metal film. In a plasmonic interferometer the metallic film is a noble metal (such as gold) and we measure directly the intensity of these interferences I_o,

Table 1. Optimized thicknesses for the metallic layers of the SPR and the MP interferometer.

Wavelength	X Au (nm) SPR	Y Co (nm) MP interferometer
550	32	5
600	42	5
633	46	6
650	47	6
750	50	6
850	49	8
950	47	10

while for MP interferometry a thin ferromagnetic film (such as Co) is inserted to allow magnetic modulation, and we measure the magnetically modulated interferences intensity I_{mp}.

2.1. Metal thickness optimization

As can be seen in figure 1 and has been briefly explained above, the three sensors use different metallic layers. To perform a fair comparison, we have theoretically optimized the thickness of the metallic layers for each configuration and wavelength using the same noble metal, Au, in the three cases. The optimized parameters appear in table 1. For conventional SPR, we have chosen SF10 glass ($n_{\mathrm{SF10}} = 1.73$) as substrate and we have calculated the Au layer thickness that provides the optimum SPP excitation, which is that providing the reflectivity closer to zero under ATR configuration at the SPP angle excitation. The obtained Au thickness values range from 32 to 50 nm. In the case of plasmonic interferometry, we need an optically opaque gold layer, so an appropriate thickness is 200 nm Au layer [33] independently of the wavelength. Finally for the MP interferometer, we look for the maximum magnetically induced modulation, which is controlled by the thickness and position of the Co layer. The optimum position of the Co layer is as close to the surface as possible, but this will cause oxidation so we have fixed it at 10 nm, which is a reasonable value to prevent oxidation in sensing aqueous environment. The complete metallic multilayer for the MP interferometers is then 180 nm Au/Y nm Co/10 nm Au, where the thickness of the cobalt layer varies from 5 to 10 nm.

2.2. Sensing layer

Sensing can be performed in different environments depending on the analyte. One of the most commonly used ones, mainly in biosensing, is an aqueous solution. Although each analyte and sensing protocol requires a specific geometry of the sensing layer, in our theoretical study we have chosen two generic situations that reproduce two of the most common configurations: two-dimensional ('surface') immobilization of biorecognition elements [7] and absorption of the analyte in a three-dimensional matrix ('bulk') [7, 34]. Figure 2(a) represents the theoretically simulated 'bulk' configuration that consists of a 80 nm layer of hydrated carboxymethyl dextran, an hydrogel used for biosensing with gold in SPR and whose refractive index in aqueous solution is 1.36 [5, 35]. A sensing experiment will be then simulated as a uniform 80 nm medium whose refractive index is varied from its original refractive index $n_0 = 1.36$ up to

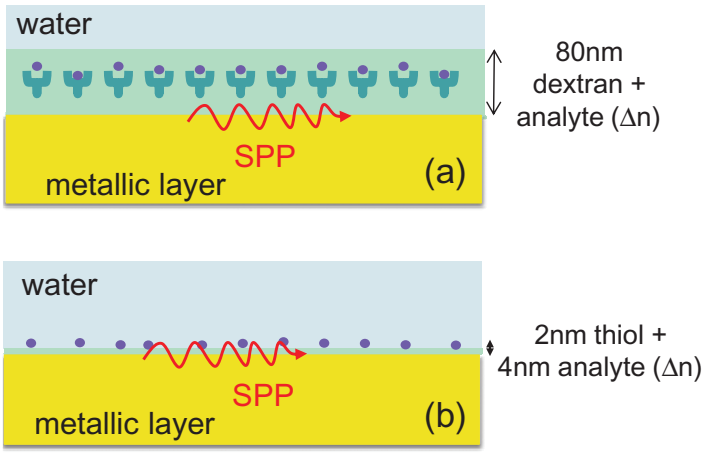

Figure 2. Simulated sensing configurations. (a) 'Bulk' system: metallic layer covered by a 80 nm dextran layer (represented by antigen–antibody pairs) immersed in water solution. (b) 'Surface' system: metallic layer covered by a 2 nm thiol layer and a 4 nm analyte layer (represented by small molecules) immersed in water solution.

1.363 ($\Delta n = 3 \times 10^{-3}$), mimicking the changes induced by the presence of an attached analyte. On the other hand, the 'surface' configuration, shown in figure 2(b), consists of a 2 nm self-assembled monolayer of thiol (a standard ligand with $n = 1.5$) with a uniform 4 nm overlayer whose refractive index will vary from 1.33 (water) up to 1.333, mimicking the adhesion of molecules such as streptavidin to the thiol layer.

2.3. Methodology

Finally, the three analysed sensing techniques use different sensor outputs, which makes their comparison subtle. We will focus on the sensitivity of the sensor, i.e. the dependence of the measured output, O, with the refractive index of the dielectric medium, n. In a plasmonic system, the sensitivity can be described as [6, 36]

$$S \equiv \frac{\mathrm{d}O}{\mathrm{d}n} = \frac{\partial O}{\partial k_{\mathrm{sp}}} \frac{\partial k_{\mathrm{sp}}}{\partial n}. \tag{1}$$

In this expression, together with the sensor output and n, it also appears that the physical parameter is being modified by the change in the refractive index, which in a plasmonic sensor usually corresponds to the SPP wavevector, k_{sp}. In fact, (1) shows that the sensitivity S can be decomposed in two terms: the variation of the actual output measured in the experiment with the physical parameter; and the variation of this physical parameter with the refractive index. The first term is dependent on the measurement method, whereas the other term depends on the used materials and geometry and the properties of the associated SPP. In order to differentiate the effect on the sensitivity ascribed to the measuring technique from those related to the properties of the physical parameter, in our comparison we will analyse separately the second term and the complete dependence of O regarding n for the three sensors. Moreover, as SPP properties depend on the wavelength, we will perform this comparison for different wavelengths.

3. Surface plasmon resonance (SPR) versus plasmonic interferometer

3.1. Dependence of k_{sp} on n

We will start our analysis comparing the SPR performance with that of the plasmonic interferometer. Both sensors are based on SPPs, which are evanescent waves that propagate along a metal–dielectric interface and are defined by its wavevector, k_{sp}. For an interface of two semi-infinite materials, k_{sp} is expressed as [37]

$$k_{sp} = k_0 n_{diel} \sqrt{\frac{\varepsilon_m}{\varepsilon_m + n_{diel}^2}}, \tag{2}$$

where k_0 is the wavevector of light in vacuum, n_{diel} the refractive index of the dielectric material and ε_m the dielectric constant of the metal. When the refractive index of the dielectric material (our sensing layer) changes from n_0 to n, the physical parameter involved in both techniques is therefore the SPP wavevector, whose modification can be expressed as

$$\Delta k_{sp} = k_{sp}(n) - k_{sp}(n_0) = \frac{\partial k_{sp}}{\partial n} \Delta n, \tag{3}$$

where $\Delta n = n - n_0$.

Equation (2) can only be applied to an interface composed of two semi-infinite materials, but given the evanescent nature of the SPP it is a good approximation for the thick metallic layer of the plasmonic interferometer. However, for the thin layer composing the SPR sensor, the SPP is affected by the presence of the substrate and its wavevector is slightly different (no analytical expression for k_{sp} can be obtained in this case, it has to be calculated numerically). As the wavevectors are different for the thin and thick metal film cases, the sensitivity of k_{sp} for the two sensing systems may also differ. Moreover, we have analysed both the 'surface' and 'bulk' configurations in order to investigate possible differences in the SPP spreading across the sensing layer between the two systems, which would affect their sensitivity differently for the two situations. Besides, being the dielectric constant of metals dispersive, k_{sp} and consequently its sensitivity also depend on wavelength.

The analysis of the sensitivity of the SPP wavevector ($\frac{\partial k_{sp}}{\partial n} = \frac{\Delta k_{sp}}{\Delta n}$ for small Δn) for both techniques as a function of the wavelength, for both 'bulk' and 'surface' configurations, is shown in figure 3. It can be seen that the two techniques present a quite close sensitivity in both 'surface' and 'bulk' configurations. The 'bulk' configuration is more sensitive than the 'surface' one, as expected [7] since the spreading of the SPP is much larger than the sensed region for the 'surface' system. However, the important result here is that the sensitivity is the same for the two analysed techniques in each sensing system, meaning that both metallic layers are equally appropriate for sensing bulk changes or surface ones. Regarding the wavelength dependence, both techniques show the same behaviour: the SPP wavevector change with Δn increases for lower wavelengths, as the SPP wavevector does [7, 37].

In summary, the physical parameter involved in both SPR and plasmonic interferometry, k_{sp}, shows the same sensitivity in both cases. However the final sensitivity of a sensing technique also depends on how the variation of k_{sp} is translated into a variation of the measured parameter O, as stated by (1). In the following we will thus analyse the sensitivity of O.

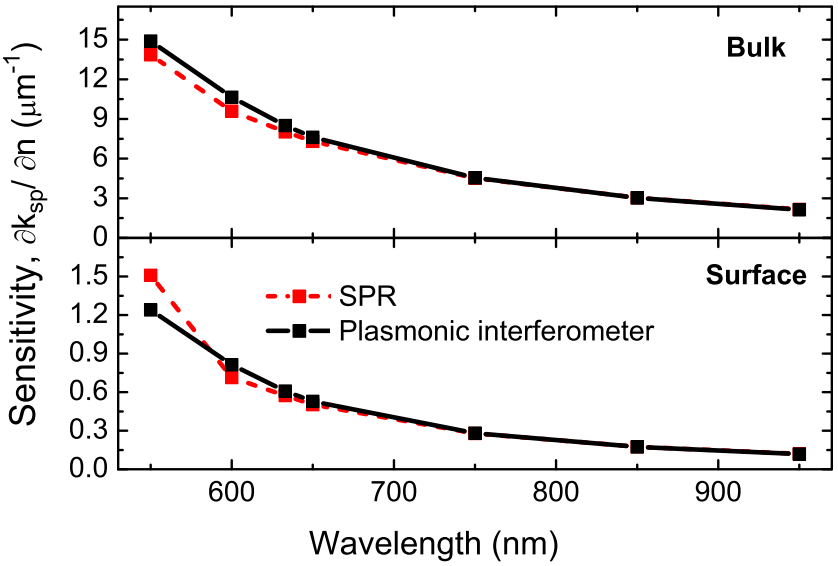

Figure 3. Sensitivity to the refractive index of the SPP wavevector ($\frac{\partial k_{sp}}{\partial n}$) for the SPR (red dashed line) and the plasmonic interferometer (black solid line) as a function of the wavelength. Both 'bulk' (upper graph) and 'surface' (lower graph) configurations are shown.

3.2. Dependence of O with n: SPR

The SPR technique, as explained briefly in section 2, measures the reflectivity R when exciting the SPP in ATR configuration. To do this, a semi-circular prism is usually set in contact with the metal, as shown in figure 1(a). For the surface plasmon to be excited, the angle of incidence of the light, θ, must fulfil $k_{sp} = k_0 n_p \sin\theta$, with n_p being the refractive index of the prism ($n_p = 1.73$ in our simulations). Therefore, when measuring the reflectivity as a function of θ, a minimum appears when the SPP is excited.

In a sensing experiment, the position of this minimum changes when n varies, due to the associated modification of the plasmon wavevector. In figure 4(a) we present a series of reflectivity curves, calculated in an exact way by our transfer matrix formalism, for different refractive indexes of the sensing layer at a given wavelength $\lambda_0 = 633$ nm. The change in the reflectivity minimum with n can be clearly seen.

A typical procedure in a SPR experiment is to monitor the reflectivity under varying conditions that modify n (e.g. with and without analyte) for a fixed set of wavelength and angle

$$\Delta R = R(n) - R(n_0). \tag{4}$$

We would like to note here that measuring the variation of the reflectivity (which is the method explained here) is not the only procedure for SPR. It can also be done otherwise, by measuring the shift in the angle of minimum reflectivity, or by analysing the reflectivity as a function of the wavelength for a given angle, and measuring the wavelength shift of the minimum of the reflectivity. However, there are studies that show that the final sensitivity of the SPR technique is independent of the measurement procedure [36], being in all cases affected by the experimental noise in the same manner. Thus the only differences when comparing

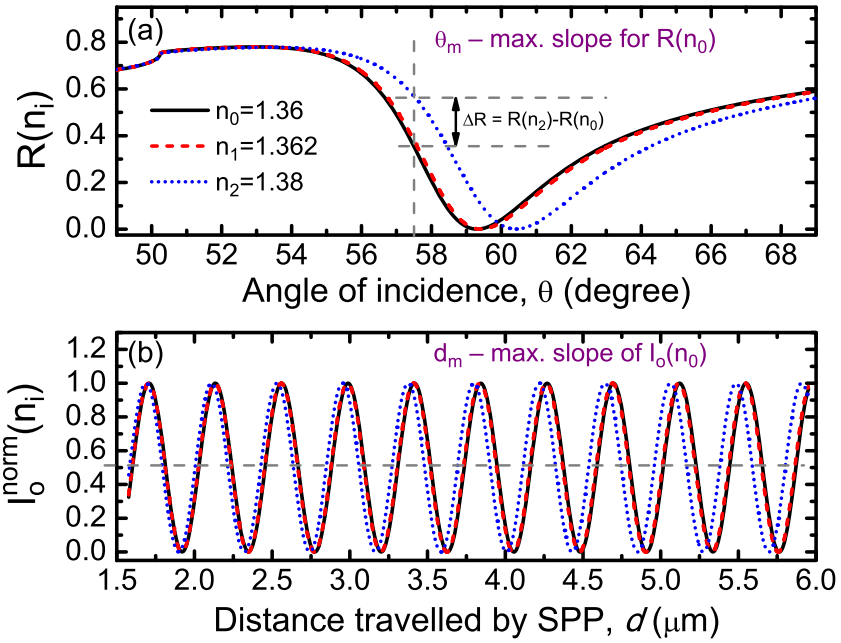

Figure 4. (a) Reflectivity as a function of the angle of incidence for different refractive index n_i in a standard SPR setup. (b) Intensity of the plasmonic interferometer, normalized to the amplitude of the oscillations, as a function of the distance d travelled by the plasmon for different refractive index n_i. In the calculation, both I_r (directly transmitted light contribution) and I_{sp} (SPP contribution) are taken to be equal. Both graphs correspond to $\lambda_0 = 633$ nm.

the different procedures are due to the precision of the apparatus. As we cannot take this into account in a theoretical paper, we are going to limit our analysis to the above described reflectivity variation procedure for SPR, without loss of generality. To obtain the maximum sensitivity with this procedure, it is necessary to carefully choose the angle of measurement, θ_m: the maximum ΔR is obtained for the angle that maximizes the slope of the R versus θ curve (see figure 4(a)).

To obtain insight on the evolution of the reflectivity with n, we can approximate the resonance dip by a Lorentzian curve [36, 38] (this approximation holds quite accurately when $|\mathrm{Re}(\varepsilon_m)| \gg n_{diel}^2$ and the metal has low losses, i.e. $\mathrm{Im}(\varepsilon_m) \ll |\mathrm{Re}(\varepsilon_m)|$). The reflectivity around the SPP dip can be written as

$$R = 1 - \frac{4\gamma_i\gamma_r}{(k_0 n_p \sin\theta - k_{sp})^2 + (\gamma_i + \gamma_r)^2}, \tag{5}$$

where γ_i and γ_r are the SPP absorption and radiation damping coefficients, respectively [38], and are responsible of the SPP dip width. The angle of measurement can be obtained after equation (5) by looking for the angle of maximum slope

$$\theta_m = \arcsin\left(\frac{k_{sp} \pm [(\gamma_i + \gamma_r)/\sqrt{3}]}{k_0 n_p}\right). \tag{6}$$

Thus, ΔR ($\equiv (\partial R/\partial n)\Delta n$ for small Δn) at θ_m is given by

$$\Delta R = \frac{3\sqrt{3}}{2}\frac{\gamma_i\gamma_r}{(\gamma_i+\gamma_r)^3}\Delta k_{sp}. \tag{7}$$

In the case when $\gamma_i = \gamma_r$, it can be seen from (5) that the reflectivity value at the minimum is zero, which is also the condition for optimum SPP excitation [38] that we have employed to define the optimum metal thickness for SPR sensors (see section 2.1). Then, ΔR can be rewritten as

$$\Delta R = \frac{3\sqrt{3}}{16\gamma_i}\Delta k_{sp}. \tag{8}$$

These two last equations, although they are not exact, indicate that the sensitivity of the SPR, $\Delta R/\Delta n$, is related to both the sensitivity of k_{sp} and a term related to the width of the reflectivity dip.

3.3. Dependence of O with n: plasmonic interferometry

There are several geometries to implement a plasmonic interferometer, such us using parallel slits [18, 19], parallel slit and groove [15–17, 21, 23, 24], tilted groove and slit [20, 22, 29, 30, 33]...etc. Nevertheless all the configurations are intrinsically equivalent. In our simulations, the employed geometry is based on a tilted groove–slit pair (see figure 1(b)), and is similar to that described in [29, 30, 33]. When radiative light illuminates the interferometer, the plasmon is launched at the groove and it travels towards the slit, where it decouples again into radiation. This radiation, together with part of the incident light, traverse the slit and produce interferences at the back side of the interferometer. The transmitted intensity at a given position in a plasmonic interferometer can then be described as [29, 30]

$$I_o = I_r + I_{sp} + 2\sqrt{I_{sp}}\sqrt{I_r}\cos(k_{sp}d + \varphi_0), \tag{9}$$

where I_r and I_{sp} are constants that account for the intensity of the two interfering waves, d is the distance travelled by the plasmon (i.e. the slit–groove distance at that point) and φ_0 is an arbitrary phase that depends on the light to plasmon conversion and vice versa. Figure 4(b) shows the interferogram obtained by recording the transmitted intensity along the slit. The intensity has been normalized to the amplitude of the oscillations ($\equiv ({I_o}^{MAX} - {I_o}^{min}) = 4\sqrt{I_{sp}}\sqrt{I_r}$). The contrast of this interferogram is maximized when I_r and I_{sp} have the same value, which can be achieved by tuning the position of the incident light regarding the slit–groove pair and the efficiency of the SPP excitation at the groove [39, 40]. When the refractive index, and therefore the SPP wavevector, change, the interferogram is shifted.

Similarly to the SPR system, both changes in the intensity at a fixed position and shifts in the position of the minima–maxima can be employed as the sensor output O without affecting the intrinsic sensitivity of the system. In this paper, we have selected the variation with the refractive index of the transmitted intensity I_o at a fixed slit position as the quantity monitored for sensing

$$\Delta I_o = I_o(n) - I_o(n_0). \tag{10}$$

Again, in order to attain the highest sensitivity, the optimum position for measuring the changes of I_o is that of the maximum slope of the I_o versus d curve.

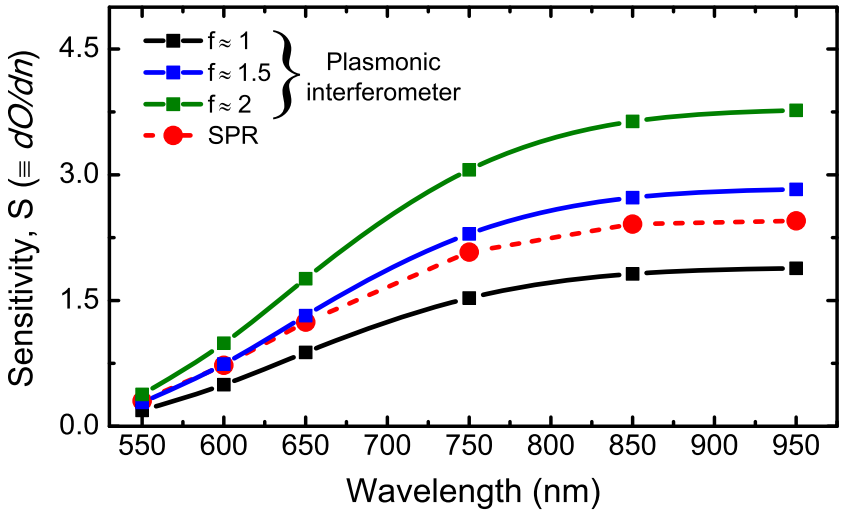

Figure 5. Sensitivity of the SPR ($S = \Delta R/\Delta n$) and the plasmonic interferometer ($S = \Delta I_0^{\text{norm}}/\Delta n$) sensors as a function of the wavelength. The calculations have been performed in the 'surface' sensing configuration, taking the optimum Au thickness for each wavelength and kind of sensor (200 nm for the plasmonic interferometer and the values collected in table 1 for the SPR). For the plasmonic interferometer, the sensitivity for various slit–groove distances, expressed in terms of $f = d/L_{\text{sp}}$, is shown.

If we neglect the attenuation of the SPP while propagating (i.e. if we consider the imaginary part of the plasmon wavevector to be very small), the variation of I_{o} due to the change of the refractive index in the sensing layer, normalized to the amplitude of the measured interferogram, can be written to first order approximation as

$$\Delta I_{\text{o}}^{\text{norm}} \equiv \frac{\Delta I_{\text{o}}}{4\sqrt{I_{\text{sp}}}\sqrt{I_{\text{r}}}} \approx -1/2\ \Delta k_{\text{sp}}\, d\ \sin(k_{\text{sp}}\, d + \varphi_0). \tag{11}$$

As can be seen in equation (11), the sensitivity of the plasmonic interferometer, $S = \Delta I_{\text{o}}^{\text{norm}}/\Delta n$, is proportional to $\Delta k_{\text{sp}} \times d$, i.e. to the sensitivity of k_{sp} times the distance travelled by the SPP. As this distance can be chosen when fabricating the device, in this sensor we have an external method to increase its sensitivity (see figure 4(b)). The distance travelled by the plasmon can be expressed in terms of the SPP propagation length, L_{sp}, which corresponds to the distance travelled by the plasmon so that its intensity becomes attenuated in a $1/e$ factor [37]. For a plasmonic interferometer, where the Au layer is very thick, the SPP damping is due only to metal absorption, so that $L_{\text{sp}} = 1/(2\gamma_{\text{i}})$ [38]. By expressing d in units of L_{sp}, $d = f \times L_{\text{sp}}$, (11) becomes

$$\Delta I_{\text{o}}^{\text{norm}} \approx \frac{-1}{4\gamma_{\text{i}}}\ f\ \Delta k_{\text{sp}}\ \sin\left(\frac{k_{\text{sp}}\ f}{2\gamma_{\text{i}}} + \varphi_0\right). \tag{12}$$

3.4. Comparison of the sensitivity for SPR and plasmonic interferometry

Figure 5 compares the evolution of S with the wavelength for both SPR and plasmonic interferometer sensors in the case of the 'surface' sensing configuration. For the plasmonic

interferometer, different values of d are considered. Plasmonic interferometry proves to be more sensitive than SPR for long enough d, because its sensitivity increases linearly with the distance travelled by the plasmon (equations (11) and (12)). The plasmonic interferometer sensitivity surpasses that of the SPR sensor for $d \geqslant 1.5L_{sp}$ in all the analysed spectral range relevant for sensing ($\lambda_0 \geqslant 600$ nm). In fact, this result can also be obtained by comparing equations (8) and (12). Moreover, this slit–groove distance is small enough to keep a good contrast in the interferogram. We estimate that the maximum reasonable value of d is that which provides a minimum interferogram contrast of 0.3 in order to clearly resolve the oscillations. Assuming $I_r = I_{sp}$, this results in $d \leqslant 2L_{sp}$. This implies that, by choosing the appropriate slit–groove distance, the performance of plasmonic interferometers for sensing can beat that of the conventional SPR.

Moreover, figure 5 also shows that the sensitivity increases with the wavelength for both kinds of sensors. This behaviour, opposite to the results presented in figure 3, reflects the fact that the final sensitivity of a sensor depends not only on the sensitivity of the physical parameter but also on other factors associated with the measured quantity. So, in the case of the SPR sensor, the width of the reflectivity resonance dip also influences S (see equations (7) and (8)). Since this width decreases strongly with the wavelength, the sensitivity of a SPR system increases at higher wavelengths even though the sensitivity of the physical parameter k_{sp} decreases (figure 3). Regarding plasmonic interferometry, the SPP propagation length L_{sp} augments rapidly with the wavelength, and being S proportional to the distance travelled by the plasmon (equations (11) and (12)), this counteracts the tendency of k_{sp}.

4. Plasmonic versus magnetoplasmonic interferometry

4.1. Evolution of k_m with n

The MP interferometer, as briefly mentioned in section 2, is based on magnetically modulating the plasmon wavevector [29, 30]. For that, a thin ferromagnetic metallic layer is introduced within the Au thick film, as shown in figure 1(c). This ensures the presence of a sizable magnetic effect and that the plasmon propagating distance is not dramatically reduced due to the higher absorption of Co. When a magnetic field is applied to the MP interferometer in the direction parallel to the surface and perpendicular to the SPP propagation direction, the SPP wavevector is modified as follows [29]:

$$k_{sp}(n, M) = k_{sp}(n, 0) + k_m(n, M), \tag{13}$$

where $k_{sp}(n, M)$ and $k_{sp}(n, 0)$ denote the SPP wavevectors in the presence or absence of sample magnetization, respectively, and $k_m(n, M)$ represents the magnetic field induced modification of the SPP wavevector. Although the absolute value of k_m is four orders of magnitude smaller than that of k_{sp} [41], it can be easily measured when using a plasmonic interferometric configuration and inverting synchronously an external magnetic field strong enough to magnetically saturate the Co layer [29, 30, 41].

When the refractive index changes, both k_{sp} and k_m are modified and therefore the two physical parameters should be taken into account when analysing the performance of the MP interferometer as a sensor. The general expression for S in this case becomes

$$S = \frac{dO}{dn} = \frac{\partial O}{\partial k_{sp}} \frac{\partial k_{sp}}{\partial n} + \frac{\partial O}{\partial k_m} \frac{\partial k_m}{\partial n}. \tag{14}$$

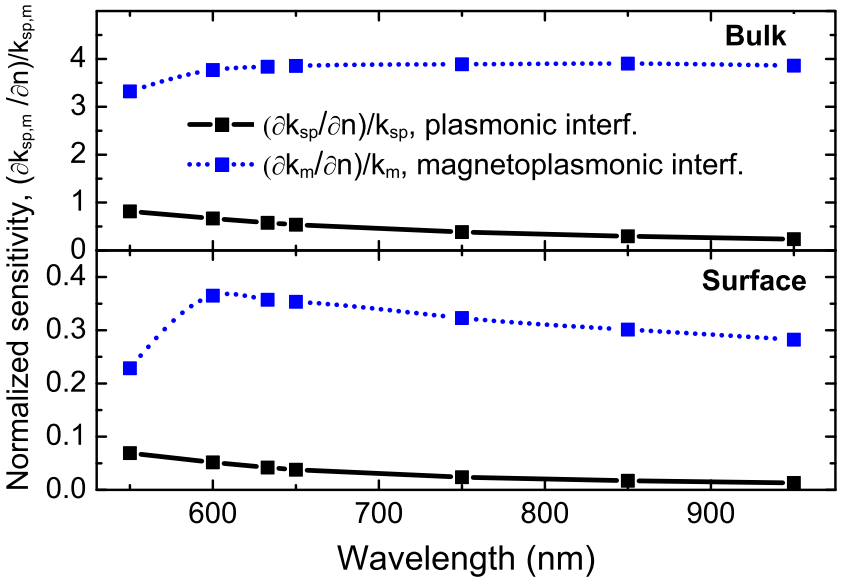

Figure 6. Sensitivity as a function of the wavelength of the normalized SPP wavevector, $\Delta k_{\mathrm{sp}}/k_{\mathrm{sp}}$, for a plasmonic interferometer (black solid line) and of the normalized SPP wavevector magnetic modulation, $\Delta k_{\mathrm{m}}/k_{\mathrm{m}}$, for a MP one (blue dotted line). For each kind of interferometer and wavelength, the optimum metal thickness has been taken. Both 'bulk' (upper graph) and 'surface' (lower graph) configurations are shown.

Analogously to Δk_{sp}, the variation of k_{m} when the refractive index of the sensing layer is modified is defined as

$$\Delta k_{\mathrm{m}} = \frac{\partial k_{\mathrm{m}}}{\partial n}\Delta n \equiv k_{\mathrm{m}}(n, M) - k_{\mathrm{m}}(n_0, M). \tag{15}$$

Figure 6 shows the evolution of the relative changes of Δk_{sp} and Δk_{m} with the wavelength for the plasmonic and the MP interferometers (note that here we need to compare the relative changes of both quantities, and not their absolute values, as these ones differ in several orders of magnitude as mentioned above). The comparison of both quantities offers an interesting result: $\Delta k_{\mathrm{m}}/k_{\mathrm{m}}$ is one order of magnitude bigger than $\Delta k_{\mathrm{sp}}/k_{\mathrm{sp}}$. This is due to the fact that the magnetic field induced modulation of the SPP wavevector has a strong dependence on the fourth power of the refractive index of the dielectric [30, 41]. As a consequence, it is to be expected that a sensing technique relying on the measurement of the variations of k_{m} exceeds in sensitivity that based on variations of k_{sp}.

From figure 6 it can also be seen that, for both 'surface' and 'bulk' sensing configurations, the relative sensitivity of the magnetic parameter surpass by one order of magnitude that of the purely plasmonic one. Regarding the spectral behaviour, except for the smallest wavelength value shown, $\Delta k_{\mathrm{m}}/k_{\mathrm{m}}$ decreases with the wavelength but in a slower manner than Δk_{sp}, and indeed for the 'bulk' configuration it can be considered as nearly constant.

4.2. Dependence of O with n: magnetoplasmonic interferometry

From the previous analysis of Δk_{m}, the MP interferometer seems a promising candidate for developing a sensor. However, care has to be taken in selecting the appropriate measured

quantity. As mentioned above, a magnetic field applied to the MP interferometer modifies the SPP wavevector, which induces a shift in the transmitted intensity interferogram (see (9)). If the magnetic field is reversed, both the SPP wavevector modification and the shift take place in the opposite direction. Therefore, when applying an alternating magnetic field, the transmitted intensity I_o is modulated synchronously with it. This modulation of the intensity, named magnetoplasmonic intensity, I_{mp}, can be expressed in first approximation as

$$I_{mp} = -4\sqrt{I_{sp}}\sqrt{I_r}k_m d \ \sin(k_{sp}d + \varphi_0) \tag{16}$$

if we neglect again the imaginary part of k_{sp}, and considering $k_m d \ll 1$ [29, 30, 41]. We would like to note that, for the optimization of the MP interferometer described in section 2.1, the quantity we have maximized is I_{mp}: as this quantity is proportional to $k_m \times d$, we have indeed maximized the product $k_m \times L_{sp}$ (as L_{sp} limits the maximum value of d that can be used).

One option for using the MP interferometer as a sensor would be the monitorization of I_{mp} at a fixed slit point when the refractive index changes. The variation of this intensity, normalized to its initial amplitude ($\equiv I_{mp}^{MAX}(n_0) - I_{mp}^{min}(n_0) = 8\sqrt{I_{sp}}\sqrt{I_r}\, k_m(n_0)\, d$), can be expressed in first order as

$$\begin{aligned}\Delta I_{mp}^{norm} &\equiv \frac{I_{mp}(n) - I_{mp}(n_0)}{8\sqrt{I_{sp}}\sqrt{I_r}\, k_m(n_0)\, d} \\ &\approx -1/2\left[\Delta k_{sp}\, d\cos(k_{sp}\, d + \varphi_0) + \Delta k_m/k_m \sin(k_{sp}\, d + \varphi_0)\right] \\ &= -1/2\sqrt{(\Delta k_{sp}\, d)^2 + (\Delta k_m/k_m)^2}\ \sin(k_{sp}\, d + \varphi_0 + \gamma),\end{aligned} \tag{17}$$

where $\tan\gamma = \frac{\Delta k_{sp} d k_m}{\Delta k_m}$. Equation (17) shows that in fact the MP interferometer is more sensitive than an equivalent plasmonic one. Nevertheless, we should analyse this statement very cautiously. As in the case of the plasmonic interferometer for I_o, the sensitivity of I_{mp} depends on the product $\Delta k_{sp} \times d$, and therefore the sensitivity can be boosted by increasing the slit–groove distance. This distance is however limited by the SPP propagation distance and, as discussed above, values of d longer than $2L_{sp}$ will result in too reduced a contrast for comfortable measurements. If we impose this limit of $d \leqslant 2L_{sp}$, the sensitivity of the plasmonic interferometer surpasses that of the MP one as the presence of Co in the metallic trilayer, highly absorbent, strongly reduces the value of L_{sp}. This is shown in figure 7, where the sensitivity of the plasmonic interferometer, relying on the measurement of I_o^{norm}, is compared with that of the MP interferometer based on the monitorization of I_{mp}^{norm}. The sensitivity of a plasmonic interferometer with $d = L_{sp}$ is higher than that of the MP one with $d = L_{sp}$ or even $d = 2L_{sp}$ due to the smaller value of L_{sp} in this last case (see inset in the figure with the evolution of L_{sp} with the wavelength for the two kind of interferometers). Furthermore, even for a MP interferometer with d equal to the value of L_{sp} corresponding to the pure Au layer composing the plasmonic one, the sensitivity of I_{mp}^{norm} is comparable or smaller than that of I_o^{norm} (compare light blue dotted line and black solid line in figure 7). This is due to the fact that the introduction of the Co layer in the MP interferometer also reduces the value of Δk_{sp}, therefore losing the increase provided by the extra term $\Delta k_m/k_m$ in (17).

The alternative of implementing the MP interferometer by monitoring the shifts in the I_{mp} interferogram is not useful for taking advantage of the higher sensitivity of k_m with respect to k_{sp} either, as the shift is only related to Δk_{sp} (see (16)). A last option that could offer the advantage of higher sensitivity for the MP interferometer is based on the direct monitorization of k_m. For that, both the transmitted intensity without a magnetic field applied and the modulated intensity

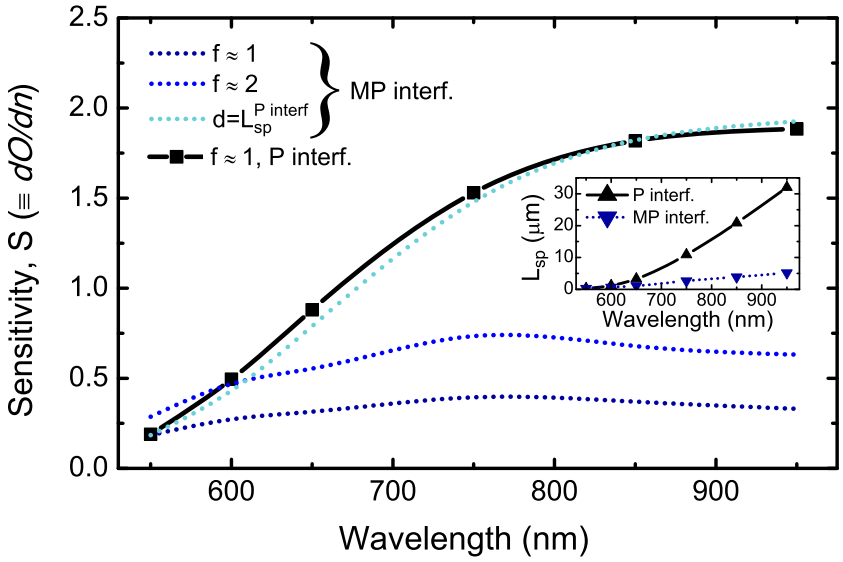

Figure 7. Calculated sensitivity of the measured intensity for the plasmonic ($S = \Delta I_{\mathrm{o}}^{\mathrm{norm}}/\Delta n$) and the MP ($S = \Delta I_{\mathrm{mp}}^{\mathrm{norm}}/\Delta n$) interferometers as a function of the wavelength. The calculations have been performed in the 'surface' sensing configuration, taking the optimum metal thickness for each wavelength and kind of interferometer (200 nm Au for the plasmonic interferometer and 180 nm Au/Ynm Co/10 nm Au, with the Y values collected in table 1 for the MP one). For the MP interferometer, the sensitivity for various slit–groove distances is shown, expressed in terms of $f = d/L_{\mathrm{sp}}$. The light blue dotted line corresponds to the sensitivity of the MP interferometer for a d value equal to the L_{sp} propagation distance of the plasmonic interferometer at the given wavelength. The inset shows the L_{sp} values at different wavelengths for the plasmonic and MP interferometers.

Table 2. Parameters involved in the three different sensing systems analysed.

Sensing method	Physical system	Physical parameter	Measured quantity
SPR	Thin Au film	Δk_{sp}	ΔR
Plasmonic interf.	200 nm Au layer	Δk_{sp}	ΔI_{o}
MP interf.	200 nm AuCoAu trilayer	Δk_{sp} and Δk_{m}	ΔI_{mp}

have to be collected for a full oscillation, and by normalizing I_{mp} to the amplitude of the full oscillation of I_{o} and dividing by the slit–groove distance, the value of k_{m} is obtained [30, 41]. This full process should be repeated when the refractive index of the sensing layer changes to obtain the new value of k_{m}. This option, although feasible, requires more signal processing and time acquisition, so it could impose some time restrictions in the sensing experiments. However, the higher sensitivity of k_{m} to the refractive index variations could compensate for this drawback.

5. Conclusions

To summarize, the sensitivity of three plasmonic-based sensing devices have been compared: standard SPR technique, plasmonic interferometry and MP interferometry. Every system has been considered at its best material implementation, and both the sensitivity of the physical parameter on which the method is based and the actual sensor output have been studied. Table 2 provides a summary of all the relevant parameters for each sensor.

Both SPR and plasmonic interferometry rely on the modification of the SPP wavevector under refractive index variations. Given that the physical system supporting each of them is very similar, i.e. Au films, there are not significative differences regarding the sensitivity of the SPP wavevector in both cases, neither in a 'bulk' sensing configuration or in a 'surface' one. When analysing the measured output, however, it has been shown that the plasmonic interferometer can surpass the SPR in sensitivity. This is due to the fact that the sensitivity of the plasmonic interferometer is proportional to the slit–groove distance, so by increasing this distance the sensitivity can be enhanced. Even though the slit–groove distance is enlarged to improve the plasmonic interferometer sensitivity, it is still kept on the order of a few tens of microns, which allows its integration in a chip for the development of miniaturized sensors. Regarding the MP interferometer, two physical parameters are involved in a sensing experiment: the modification of the SPP wavevector and the variation of the magnetic field driven SPP wavevector modulation. This last quantity has a stronger dependence with the refractive index than Δk_{sp}, so a sensor based on it would provide a higher performance. However, in order to take advantage of this, the monitored output quantity in a MP interferometer has to be directly the processed value of k_m.

Regarding the wavelength behaviour, the sensitivity of both the SPR and the plasmonic interferometer increases with wavelength even though the variations of k_{sp} with the refractive index behave in the opposite manner. This is because of the reduced losses of the SPP at higher wavelengths, which generate narrower reflections dips in SPR sensors and allow longer values of d in the plasmonic interferometers. For the MP interferometer, on the other hand, the use of smaller wavelengths would be advantageous as Δk_m, which is the most adequate output here, decreases with the wavelength.

Acknowledgments

We acknowledge funding from the Spanish MINECO ('MAPS' MAT2011-29194-C02-01 and 'FUNCOAT' CONSOLIDER INGENIO 2010 CSD2008-00023) and the Comunidad de Madrid ('MICROSERES-CM' S2009/TIC-1476).

References

[1] Anker J N, Hall W P, Lyandres O, Shah N C, Zhao J and Van Duyne R P 2008 *Nature Mater.* **7** 442–53
[2] Svedendahl M, Chen S, Dmitriev A and Käll M 2009 *Nano Lett.* **9** 4428–33
[3] Otte M A, Sepulveda B, Ni W, Juste J P, Liz-Marzan L M and Lechuga L M 2010 *ACS Nano* **4** 349–57
[4] Homola J, Yee S S and Gauglitz G 1999 *Sensors Actuators* B **54** 3–15
[5] Schasfoort R B M and Tudos A J (ed) 2008 *Handbook of Surface Plasmon Resonance* (Cambridge: RSC)
[6] Homola J 2003 *Anal. Bioanal. Chem.* **377** 528–39
[7] Homola J 2008 *Chem. Rev.* **108** 462–93

[8] Hoa X, Kirk A and Tabrizian M 2007 *Biosens. Bioelectron.* **23** 151–60
[9] Sepulveda B, Calle A, Lechuga L M and Armelles G 2006 *Opt. Lett.* **31** 1085–7
[10] Triranjita Srivastava R D and Jha R 2011 *Sensors Actuators* B **157** 246–52
[11] Ince R and Narayanaswamy R 2006 *Anal. Chim. Acta* **569** 1–20
[12] Kussrow A, Enders C S and Bornhop D J 2012 *Anal. Chem.* **84** 779–92
[13] Prieto F, Sepulveda B, Calle A, Llobera A, Dominguez C, Abad A, Montoya A and Lechuga L M 2003 *Nanotechnology* **14** 907
[14] Bruck R, Melnik E, Muellner P, Hainberger R and Lämmerhofer M 2011 *Biosens. Bioelectron.* **26** 3832–7
[15] Gay G, Alloschery O, Viaris de Lesegno B, O'Dwyer C, Weiner J and Lezec H J 2006 *Nature Phys.* **2** 262–7
[16] Pacifici D, Lezec H J and Atwater H A 2007 *Nature Photon.* **1** 402–6
[17] Temnov V V, Woggon U, Dintinger J, Devaux E and Ebbesen T W 2007 *Opt. Lett.* **32** 1235–7
[18] Wu X, Zhang J, Chen J, Zhao C and Gong Q 2009 *Opt. Lett.* **34** 392–4
[19] Gao Y, Gan Q, Xin Z, Cheng X and Bartoli F J 2011 *ACS Nano* **5** 9836–44
[20] Li X, Tan Q, Bai B and Jin G 2011 *Opt. Express* **19** 20691–703
[21] Feng J, Siu V S, Roelke A, Mehta V, Rhieu S Y, Palmore G T R and Pacifici D 2012 *Nano Lett.* **12** 602–9
[22] Yavas O and Kocabas C 2012 *Opt. Lett.* **37** 3396–8
[23] Bian T, Dong B Z and Zhang Y 2013 *Plasmonics* **8** 741–4
[24] Gao Y, Xin Z, Gan Q, Cheng X and Bartoli F J 2013 *Opt. Express* **21** 5859–71
[25] Shin Y B, Kim H M, Jung Y and Chung B H 2010 *Sensors Actuators* B **150** 1–6
[26] Markowicz P P, Law W C, Baev A, Prasad P N, Patskovsky S and Kabashin A 2007 *Opt. Express* **15** 1745–54
[27] Regatos D, Sepúlveda B, Fariña D, Carrascosa L G and Lechuga L M 2011 *Opt. Express* **19** 8336–46
[28] Dicken M J, Sweatlock L A, Pacifici D, Lezec H J, Bhattacharya K and Atwater H A 2008 *Nano Lett.* **8** 4048–52
[29] Temnov V V, Armelles G, Woggon U, Guzatov D, Cebollada A, Garcia-Martin A, Garcia-Martin J, Thomay T, Leitenstorfer A and Bratschitsch R 2010 *Nature Photon.* **4** 107–11
[30] Martin-Becerra D, Gonzalez-Diaz J B, Temnov V V, Cebollada A, Armelles G, Thomay T, Leitenstorfer A, Bratschitsch R, Garcia-Martin A and Gonzalez M U 2010 *Appl. Phys. Lett.* **97** 183114
[31] Gonzalez-Diaz J B 2010 Magnetoplasmonics. Magnetooptics in plasmonics systems *PhD Thesis* Universidad Autonoma de Madrid, Spain
[32] Postava K, Pištora J and Višňovský Š 1999 *Czech. J. Phys.* **49** 1185–204
[33] Temnov V V, Nelson K, Armelles G, Cebollada A, Thomay T, Leitenstorfer A and Bratschitsch R 2009 *Opt. Express* **17** 8423–32
[34] Manera M G *et al* 2011 *J. Mater. Chem.* **21** 16049–56
[35] Piehler J, Brecht A, Hehl K and Gauglitz G 1999 *Colloids Surf.* B **13** 325
[36] Piliarik M and Homola J 2009 *Opt. Express* **17** 16505–17
[37] Maier S A 2007 *Plasmonics: Fundamentals and Applications* (New York: Springer)
[38] Raether H 1988 *Surface Plasmons on Smooth and Rough Surfaces and on Gratings* (*Springer Tracts in Modern Physics* vol 111) (Berlin: Springer) pp 4–16
[39] Renger J, Grafström S and Eng L M 2007 *Phys. Rev.* B **76** 045431
[40] Lalanne P, Hugonin J, Liu H and Wang B 2009 *Surf. Sci. Rep.* **64** 453–69
[41] Martin-Becerra D, Temnov V V, Thomay T, Leitenstorfer A, Bratschitsch R, Armelles G, Garcia-Martin A and Gonzalez M U 2012 *Phys. Rev.* B **86** 035118